

Thermal analysis and volume properties of the systems $(\text{LiF}-\text{CaF}_2)_{\text{eut.}}-\text{LnF}_3$ (Ln = Sm, Gd, and Nd) up to 1273 K

Jarmila Mlynáriková¹ · Miroslav Boča¹ · Veronika Gurišová¹ ·
Iveta Macková¹ · Zuzana Netriová¹

Received: 25 August 2015 / Accepted: 28 December 2015 / Published online: 20 January 2016
© Akadémiai Kiadó, Budapest, Hungary 2016

Abstract Systems $(\text{LiF}-\text{CaF}_2)_{\text{eut.}}-\text{LnF}_3$ (Ln = Sm, Gd, and Nd) were investigated by means of thermal analysis and density measurements. Temperatures of primary crystallisation were measured and solidified samples were analysed by XRD as well as by SEM images and EDX mapping of the solidified samples. Densities of individual melts were measured by hydrostatic weighting (Archimedeian method). Consequently, molar volumes were calculated. Unusual behaviour was observed in all three cases, when molar volumes decrease with initial LnF_3 additions up to 1 mol % of LnF_3 . Further LnF_3 additions result in molar volumes increase. In the case of GdF_3 system, anomalous molar volume behaviour was observed: over 1 mol % of GdF_3 molar volume is higher at lower temperatures. Partial molar volumes of LnF_3 components were analysed by both simple linear or polynomial regression and multicomponent polynomial regression using least square parameters minimisation procedure. With increasing temperature, partial molar volumes of LnF_3 decrease even to negative values.

Keywords Molten salt · Temperature of primary crystallisation · Density · Molar volume · Partial molar volume · Samarium fluoride · Gadolinium fluoride · Neodymium fluoride · Molten salts

Introduction

In the second half of previous century, the research of different molten salts systems, in general, was exhaustive concerning single salts or binary systems. Predominantly phase diagrams and, less frequent, other physico-chemical properties were analysed. Even in binary systems there is lot of obstacles: (1) relatively high melting points of majority of salts, (2) formation of glasses making measurements difficult, (3) formation of new phases that still have not been characterised, and (4) high tendency to reaction with oxygen impurities. Unless all phases formed in the system are not known and unless they are not thermo-chemically characterised, it is difficult to perform such an easy task like calculation of phase diagram (this can be partially overcome by some estimations).

Concerning the motivation to study molten systems, the most frequently considered topic is potential in solar energy storage for nitrate salts (e.g. [1–3]) or in nuclear energy production for fluoride melts (among others, e.g. topics for metallurgy). There are hundreds of reports on physico-chemical properties related to nuclear applications on different fluoride systems [4, 5]. The main problem arises from the fact that all these accessible data suffer with any systematic approach. Significant portion of these data is only in restricted composition or temperature range or only for some exact compositions. There are also significant data gaps what make any effort for data correlation impossible.

This work is related to the systems like $\text{LiF}-\text{CaF}_2-\text{LnF}_3$. Summary of physico-chemical properties of binary systems is given in Table 1. As can be seen from the table, there are no data for, e.g., density, viscosity, or other physico-chemical properties even for binary systems. Almost no experimental data for ternary systems are accessible, as

✉ Jarmila Mlynáriková
jarmila.mlynarikova@savba.sk

¹ Institute of Inorganic Chemistry, Slovak Academy of Sciences, Dúbravská cesta 9, 845 36 Bratislava, Slovakia

Table 1 Summary of physico-chemical properties of investigated binary systems

System	Measured property	Comment
LiF–LaF ₃	Phase diagram	16.7 mol % LaF ₃ ; $T_{\text{eut.}} = 1043$ K [6, 7]
LiF–GdF ₃	Phase diagram	26 mol % GdF ₃ ; $T_{\text{eut.}} = 973$ K 39 mol % GdF ₃ ; $T_{\text{per.}} = 1028$ K and $\alpha \rightarrow \beta$ 50 mol % GdF ₃ at $T_{\text{per.}} = 1148$ K [8] 25 mol % GdF ₃ ; $T_{\text{eut.}} = 971$ K and 34 mol % GdF ₃ ; $T_{\text{eut.}} = 1028$ K [9]
LiF–NdF ₃	Phase diagram	23 mol % NdF ₃ ; $T_{\text{eut.}} = 1011$ K [8]
LiF–SmF ₃	Phase diagram	27 mol % SmF ₃ ; $T_{\text{eut.}} = 971$ K [8]
CaF ₂ –LaF ₃	Phase diagram	58 mol % LaF ₃ ; $T_{\text{eut.}} = 1584$ K [10–12] 56.2 mol % LaF ₃ ; $T_{\text{eut.}} = 1585$ K [7]
CaF ₂ –GdF ₃	Phase diagram	60 mol % GdF ₃ ; $T_{\text{eut.}} = 1506$ K [10, 11, 13]
CaF ₂ –NdF ₃	Phase diagram	60 mol % NdF ₃ ; $T_{\text{eut.}} = 1557$ K [10, 11]
CaF ₂ –SmF ₃	Phase diagram	67 mol % SmF ₃ ; $T_{\text{eut.}} = 1521$ K [10, 11] 56 mol % SmF ₃ ; $T_{\text{eut.}} = 1473$ K [14]
LiF–CaF ₂ –LaF ₃	Phase diagram electrochemical investigation	15.8 mol % LaF ₃ ; $T_{\text{eut.}} = 981$ K and 17.4 mol % LaF ₃ ; $T_{\text{eut.}} = 1002$ K [7] 13.9 mol % LaF ₃ ; $T_{\text{eut.}} = 985$ K and 14.8 mol % LaF ₃ ; $T_{\text{per.}} = 1002$ K [7] [15]
LiF–CaF ₂ –GdF ₃	Electrochemical investigation	[14]
LiF–CaF ₂ –NdF ₃	Electrochemical investigation	[14, 16]
LiF–CaF ₂ –SmF ₃	Electrochemical investigation	[17]

$T_{\text{eut.}}$ is eutectic temperature and ($T_{\text{per.}}$) is peritectic temperature

well. The aim of this work is to investigate systems of (LiF–CaF₂)_{eut.}–LnF₃ (Ln = Gd, Nd, and Sm) in terms of primary crystallisation temperature measurements and volume properties analysis in the temperature range up to 1273 K in order to get some systematic data suitable for comparison.

Experimental

Chemicals

The following chemicals were used: LiF (99.9 %, Sigma-Aldrich), CaF₂ (99 %, Merck), SmF₃ (99.9 %, Chempur), NdF₃ (99.9 %, Chempur), and GdF₃ (99.9 %, Chempur). LiF was dried at 773 K during 4 h, and CaF₂ was dried at 773 K during 4 h. All chemicals were handled inside high-purity argon atmosphere (99.9990 %, Messer Tatragas) in a glove box (water content < 10 ppm).

Thermal analysis

The phase equilibria of the investigated system were determined by the means of a thermal analysis method. Detailed measuring procedure was published several times and can be found in [6–14]. All samples were homogenised and placed in a platinum crucible in glove box under inert atmosphere (Ar—Messer, 99.999 % purity). Homogenised sample (ca 7 g) in a platinum crucible was transferred into

the preheated furnace at 353 K under dried argon atmosphere (Ar—Messer, 99.996 % purity). The experiments were done in tightly closed vertical resistance furnace with water cooling (Detailed description of the experimental device is shown in Fig. 1). Thereafter the sample was heated at rates of 7 K min^{−1} up to 323–343 K above the liquidus temperature. The temperatures of phase transitions at primary and eutectic crystallisation were determined. The cooling rate was set to 1.5 K min^{−1}. The temperature control and the data processing were performed using computerised measuring device (multicomponent model for thermal analysis data collections—National InstrumentsTM, where the data collections run online under LabviewTM software), developed on our institute. The temperature of the sample was controlled by a Pt–PtRh10 thermocouple calibrated with the melting points of pure NaCl. The original figure of cooling curve of thermal analysis is shown in Fig. 2.

Density

The density of the investigated system was determined by the Archimedean method. Crucial a part of devices are precision analytical balance with automatic balancing, who are they place above furnace. A platinum vessel suspended in a platinum wire of 0.3 mm diameter, attached below an electronic balance unit, was used as the measuring body (platinum globule with diameter 15 mm and mass 34 g). The temperature dependence of the volume of the vessel

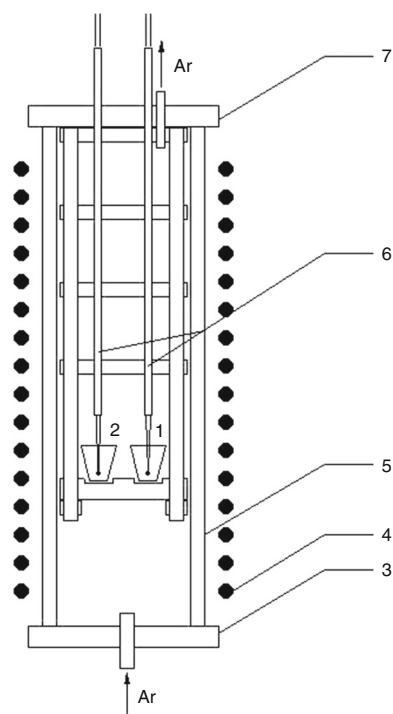


Fig. 1 Scheme of devices for measurement of the phase equilibriums. 1 Pt crucible with sample, 2 Pt crucible with reference substance (Al_2O_3), 3 bottom flange of furnace, 4 Kanthal heating element, 5 stack of furnace, 6 thermocouples, 7 top flange of furnace

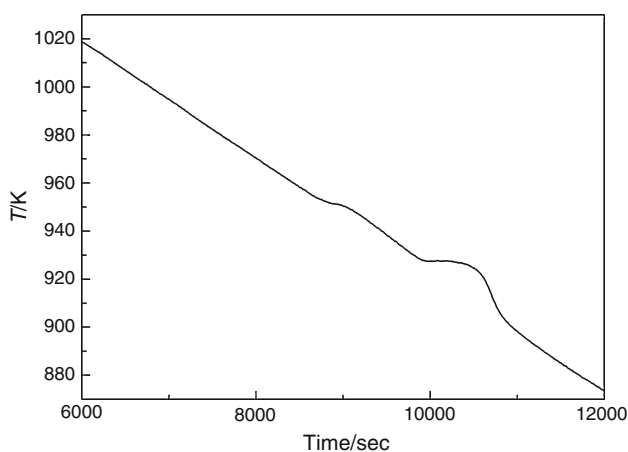


Fig. 2 Cooling curve of the system $(\text{LiF}-\text{CaF}_2)_{\text{eut.}}-\text{GdF}_3-20$ mol % GdF_3

was determined by calibration, using molten NaCl , KF , all of analytical grade purity. The temperature was measured using a Pt–Pt10Rh thermocouple calibrated at the melting points of NaCl and KF . An online PC XT computer was used for control of the measuring device and for evaluation of the experimental data. The platinum crucible (diameter 40 mm, height 50 mm) containing homogenised sample about 60–70 g [sample was homogenised in a glove box (water content < 10 ppm)] was placed inside a water-

cooled vertical resistance furnace, which was preheated at 573 K. A sample was held under an atmosphere of dried nitrogen. Position of platinum crucible was just below the measuring body. A Pt–Pt10Rh thermocouple inside the crucible was also used to indicate the melting of the sample. A scheme of the used apparatus is shown in Fig. 3.

The measurements were taken in a temperature interval depending on the temperature of primary crystallisation of the measured mixture. The samples were heated to the upper temperature (373–423 K) above the primary crystallisation. Then the measuring body was immersed into the melt, and the first set of measurements in the cooling direction was performed down to the temperature ca. 293 K above the temperature of primary crystallisation. The density results were automatically recorded by the measuring device every 3 s for each melt. A detailed description of the measuring device, calibration, and data

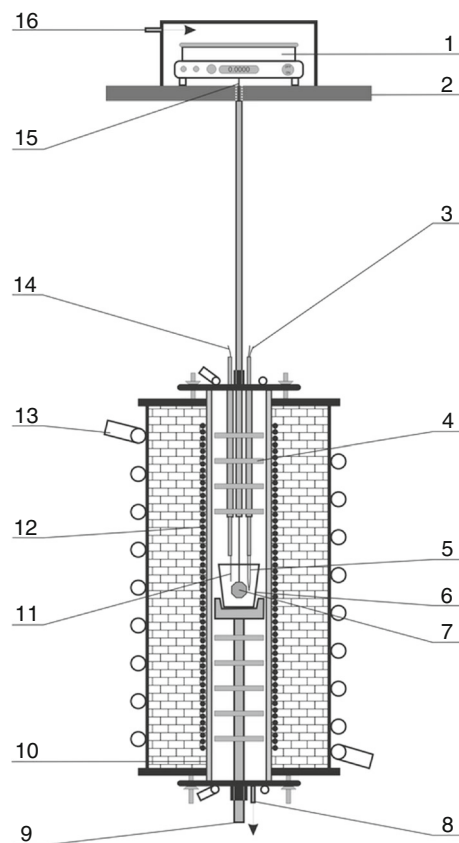


Fig. 3 Apparatus for the density measurement according to Archimedeian method. 1 Analytical balance with automatic balancing, 2 stand on analytical balance, 3 output of working Pt thermocouple, 4 radiation rings, 5 working Pt thermocouple, 6 Pt crucible, 7 measuring body, 8 output of nitrogen, 9 stand on Pt crucible, 10 stack of furnace, 11 electric contact level, 12 Kanthal heating element, 13 input of cooling water, 14 output of electric contact, 15 Pt wire, 16 input of nitrogen

manipulation was published several times elsewhere [15–19].

Powder X-ray diffraction

X-ray powder diffraction patterns of solidified samples were collected on Stoe Stadi P transmission diffractometer equipped with a curved Ge (111) monochromator placed in primary beam and a linear PSD. In order to achieve better resolution, cobalt lamp radiation was used. The records were taken in the 2θ range of $7\text{--}70^\circ$ at room temperature each for 2 h. Phase analysis was performed with X'Pert HighScore Plus PANalytical software with PDF2 2011 database.

SEM EDX

The surface morphology of the samples was analysed using a scanning electron microscope (SEM) EVO 40 (Carl-Zeiss, Germany) equipped with energy-dispersive X-ray (EDX) spectroscopy (calibrated to Cu). The samples were cut into halves, and the surface on the cut edge was analysed after the sample was covered by carbon vapours.

Results and discussion

Eutectic composition of the systems $\text{LiF}\text{--}\text{CaF}_2$ was reported several times with the following coordinates: 19.5 mol % CaF_2 $T_{\text{eut.}} = 1042\text{ K}$ [20] and 21.7 mol % CaF_2 $T_{\text{eut.}} = 1041.5\text{ K}$ [21]. In this work, the composition of 21 mol % CaF_2 was used and the measured temperature of primary crystallisation was as high as 1036 K.

For all three systems $(\text{LiF}\text{--}\text{CaF}_2)_{\text{eut.}}\text{--}\text{LnF}_3$ ($\text{Ln} = \text{Sm}, \text{Gd}, \text{and Nd}$), temperatures of primary crystallisation were measured in the temperature accessible concentration range up to $x(\text{SmF}_3) = 0.55$, $x(\text{GdF}_3) = 0.3$, and $x(\text{NdF}_3) = 0.4$, respectively, because of relatively high melting temperatures of pure salts (SmF_3 1572 K, GdF_3 1509 K, and NdF_3 1649 K [22]). All the quasi-binary systems are cross sections of the ternary systems $\text{LiF}\text{--}\text{CaF}_2\text{--}\text{LnF}_3$. In all cases, only schematic phase diagram in the measured concentration range is presented as the real calculation of curves of the primary crystallisation cannot be performed. The substantial objection for this calculation is the absence of fusion enthalpies data of particular components, and the second complication arises from the existence of new unidentified phases formed in the systems.

In all investigated systems, one must cope with the problem of phase's identification. The basic complication arises from the fact that in the PDF database of XRD patterns lot of old incorrect data are still present, and it means they are either mixtures of several compounds or

they represent different compound as is the reality. Only those XRD with known structure or those supported by the structure calculation can be considered without ambiguity. The second problem is that in the investigated systems one often get samples providing XRD patterns that cannot be matched to any known compound. Thus until the structure from single crystals or calculated structure from XRD of pure phase is not known, one is not able to identify the reaction products. This is general problem of this kind of research. Based on these shortcomings, the measured temperatures of primary crystallisation serve to estimate experimental temperature range for density measurements and will not be discussed in details.

$(\text{LiF}\text{--}\text{CaF}_2)_{\text{eut.}}\text{--}\text{SmF}_3$ system

The temperatures of primary crystallisation together with temperatures of other thermal effects are summarised in Table 2, and data are graphically shown in Fig. 4. The system $\text{LiF}\text{--}\text{SmF}_3$ seems to be simple binary one with one eutectic point [23], and the formation of any additional phases was reported neither in ICDD nor in PDF2 database. This fact is worthy of remark as in all other systems $\text{MF}\text{--}\text{SmF}_3$ ($\text{M} = \text{Na}, \text{K}, \text{Rb}, \text{and Cs}$) the formation of some other compound was reported [24, 25].

The system $\text{CaF}_2\text{--}\text{SmF}_3$ is not trivial simple binary system, but that one with the formation of different unspecified solid solution areas [26–28]. Neither in this binary system the formation of any new compounds was reported. In the quasi-binary system $(\text{LiF}\text{--}\text{CaF}_2)_{\text{eut.}}\text{--}\text{SmF}_3$, the formation of other phases fields was observed as

Table 2 Melt composition (x) of SmF_3 , temperatures of primary crystallisation (T_{PC}), together with temperatures of other thermal effects (T_1 , T_2) and hitting temperature ($T_{\text{max.}}$) of the $(\text{LiF}\text{--}\text{CaF}_2)_{\text{eut.}}\text{--}\text{SmF}_3$ system

$x(\text{SmF}_3)$	T_{PC}/K	T_1/K	T_2/K	$T_{\text{max.}}/\text{K}$
0.000	1036			
0.003	1036			1083
0.006	1036			1083
0.010	1035			1083
0.030	1031	990		1083
0.050	1024	988		1083
0.100	1009	1000	930	1083
0.150	991		932	1223
0.200	977		935	1043
0.250	968		936	1043
0.300	949		1330	1123
0.400	1046	1035	937	1223
0.500			1330	1043
0.550			936	1273

expected based on results of CaF₂–SmF₃ system. In order to estimate whether some new phases could be formed, XRD patterns of the solidified samples were recorded and summarised in Table 3. As can be seen some extra diffractions start to appear from $x(\text{SmF}_3) = 0.1$ besides the system initial components. Moreover, intensities of diffraction patterns of solidified mixtures are lower by factor of 10 in comparison with pure components showing thus lowered tendency to crystallise that can be caused by the increased tendency to form a glassy fraction. The intensity of the additional diffractions changes with the increasing content of SmF₃ indicating the formation of some new component or even more components. Final complication arises from the shift of some diffractions indicating the formation of solid solutions. Based on the actual laboratory XRD patterns, it is not possible to identify how many phases are formed in the system. It is, however, highly expected that some new phases are formed. This assumption can be supported by the vanishing of minor component of the (LiF–CaF₂)_{eut.} at high SmF₃ concentration as consequence of the interaction of these components due to the “consummation” of CaF₂ below detection limit. It must be also noted that in the solidified system the presence of SmOF was detected based on XRD measurements, most probably as a consequence of furnace inert atmosphere imperfections. LiF and CaF₂ do not undergo to any phase transformation with increasing temperature at normal pressure; however, SmF₃ undergoes to the phase transformation at 768 K from orthorhombic to rhombohedral/hexagonal symmetry [22, 29].

The temperature dependence of the density for all our investigated systems was expressed in the form of the linear equation [15–19]

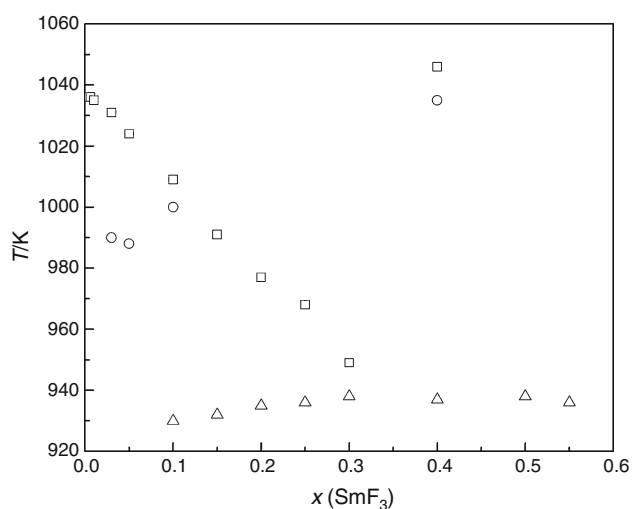


Fig. 4 Schematic phase diagram of the system (LiF–CaF₂)_{eut.}–SmF₃ with thermal effects: T_{PC} (square), T_1 (circle), T_2 (triangle): molar fraction of SmF₃ (x)

$$\rho = a - bT \quad (1)$$

where $\rho/\text{g cm}^{-3}$ is density, T/K is temperature and coefficients $a/\text{g cm}^{-3}$ and $b/\text{g cm}^{-3} \text{K}^{-1}$ are constants along with the standard deviations of approximations, obtained by the linear regression analysis of experimentally obtained data. Table 4 summarises the regression coefficients $a/\text{g cm}^{-3}$ and $b/\text{g cm}^{-3} \text{K}^{-1}$ for calculation of density of the (LiF–CaF₂)_{eut.}–SmF₃ system, and concentration dependence of density calculated based on these coefficients is shown in Fig. 5. Measured density data for the eutectic mixture (LiF–CaF₂)_{eut.} at 1173 K reported as high as 2.040 g cm^{-3} for 79 mol % LiF correspond to the reference density reported as high as 2.020 g cm^{-3} for the composition of 80 mol % LiF and temperature 1170 K [30]. With increasing initial SmF₃ content, the densities of the melts increase significantly. This increase can be characterised as “non-smooth”, and it seems to reflect interactions in the melt that can be deduced from the concentration dependence of primary crystallisation temperatures and related processes.

Some more information about the system behaviour and properties can be deduced from volume properties. We are not aware of any data neither for binary systems LiF–SmF₃ and CaF₂–SmF₃ nor for the quasi-binary system (LiF–CaF₂)_{eut.}–SmF₃.

Molar volume dependence on composition in binary systems is usually monotonic, but occasionally the presence of local minimum can occur (in the cross section of multicomponent systems, the situation can be even more complicated) [6, 11–13, 16, 17, 19, 31–33]. This is the case for all investigated systems in this work. Molar volume of (LiF–CaF₂)_{eut.}–SmF₃ initially decreases with small addition of SmF₃ up to 1 mol %. With further SmF₃ addition (up to 50 mol %), molar volume increases up to ca 50 % higher value in comparison with the initial molar volume (Fig. 6). However, the shape of the concentration dependence of molar volume indicates that over 50 mol % of SmF₃ the molar volume will increase less abruptly. Molar volume of pure molten SmF₃ was not possible to measure as its melting temperature is 1572 K [22]. It can be just estimated that molar volume of molten SmF₃ could be higher (ca 15–25 %) than its room temperature value that is as high as $31.21 \text{ cm}^3 \text{ mol}^{-1}$.

In our previous works, the calculation of compressibility parameter, ζ , provided some basic information whether volume contraction (e.g. NaF–K₂NbF₇, KF–K₂NbF₇ systems [33]) or volume expansion ((LiF–NaF–KF)_{eut.}–Na₇Zr₆F₃₁ system [6]) takes place in the system. In these systems, molar volumes monotonically increased with addition of the solute component to solvent. Compressibility parameter can be calculated according to

$$\zeta_i^T = \bar{V}_i^T - V_i^{*T} \quad (2)$$

Table 3 Phases identified in the XRD patterns of the solidified samples of the (LiF–CaF₂)_{eut.}–SmF₃ system

$x(\text{SmF}_3)$	$w(\text{SmF}_3)$	LiF	CaF ₂	SmF ₃	SmOF	Unassigned diffractions $d/\text{Å}$
1.000	1.000	–	–	+	–	–
0.010	0.054	+	+	–	+	–
0.030	0.148	+	+	–	+	–
0.050	0.228	+	+	–	+	–
0.100	0.385	+	+	+	+	1.9745
0.150	0.498	+	–	+	+	1.9760
0.200	0.584	+	–	+	–	3.2201
						2.7899
						1.9739
						1.6773
0.250	0.652	+	–	+	–	3.2283
						2.7960
						1.9766
						1.7464
0.300	0.707	+	–	+	–	3.2283
						2.7983
						1.9782
						1.7464
0.400	0.789	–	–	+	–	3.2422
						2.8080
						1.9840
0.500	0.849	–	–	+	–	3.2404
						3.0216
						2.8063
						1.9844
						1.9782

Table 4 Regression coefficients $a/\text{g cm}^{-3}$ and $b/\text{g cm}^{-3} \text{K}^{-1}$ and the standard deviations for the temperature (T/K) dependence of the density ($\rho/\text{g cm}^{-3}$) of the investigated system (LiF–CaF₂)_{eut.}–SmF₃

$x(\text{LiF–CaF}_2)_{\text{eut.}}$	$x(\text{SmF}_3)$	$a/\text{g cm}^{-3}$	$b \text{ } 10^4/\text{g cm}^{-3} \text{K}^{-1}$	T/K
1.000	0.000	2.758 ± 0.007	6.119 ± 0.059	1203–1073
0.995	0.005	2.744 ± 0.002	5.510 ± 0.014	1223–1123
0.990	0.010	2.613 ± 0.001	3.779 ± 0.012	1223–1123
0.980	0.020	2.826 ± 0.004	5.156 ± 0.033	1223–1123
0.950	0.050	2.683 ± 0.002	2.520 ± 0.015	1223–1123
0.900	0.100	3.518 ± 0.002	6.789 ± 0.019	1143–1043
0.850	0.150	3.423 ± 0.004	4.858 ± 0.030	1193–1113
0.700	0.300	4.287 ± 0.004	6.281 ± 0.033	1273–1193
0.600	0.400	4.968 ± 0.006	8.404 ± 0.045	1323–1233
0.500	0.500	5.429 ± 0.006	7.505 ± 0.039	1423–1353

where $\zeta_i^T/\text{cm}^3 \text{mol}^{-1}$ is compressibility parameter of the i th component at certain temperature. $\bar{V}_i^T/\text{cm}^3 \text{mol}^{-1}$ is partial molar volume of the added component at certain temperature (here SmF₃), and $V_i^{*,T}/\text{cm}^3 \text{mol}^{-1}$ is molar volume of

the pure added component. Partial molar volume of the binary system can be calculated according to the equation

$$\bar{V}_i^T = V_m^T + x_j \left(\frac{\partial V_m^T}{\partial x_i} \right) \quad (3)$$

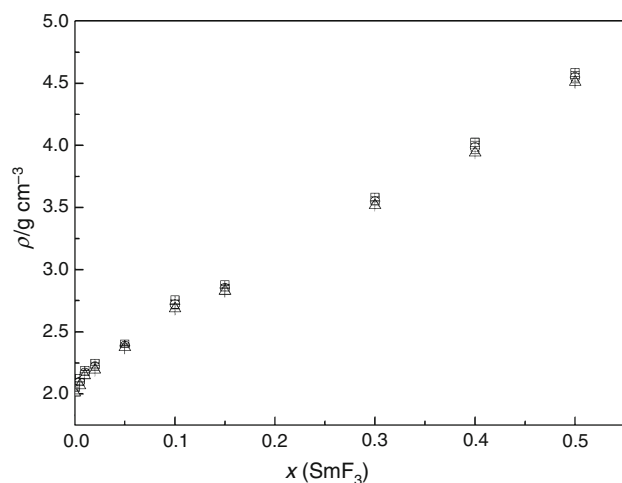


Fig. 5 Graphical representation of concentration dependence of the density ρ and the standard deviations of ρ of the molten system $(\text{LiF-CaF}_2)_{\text{eut.}}-\text{SmF}_3$ at temperature (square) 1123 K; (circle) 1173 K; (triangle) 1223 K

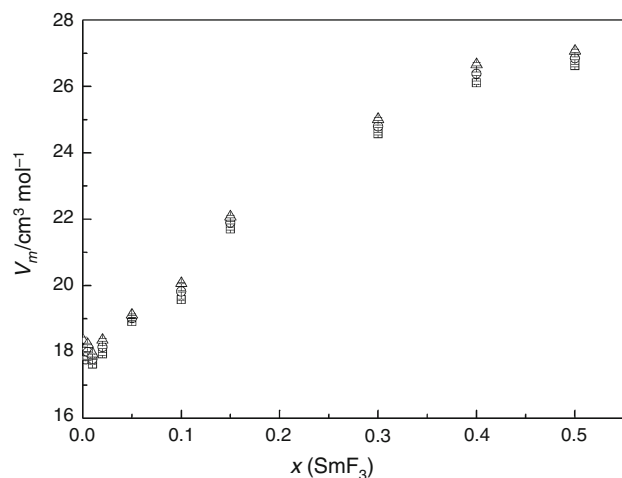


Fig. 6 Molar volume V_m and the standard deviation of V_m of the molten system $(\text{LiF-CaF}_2)_{\text{eut.}}-\text{SmF}_3$ at temperatures (square) 1123 K; (circle) 1173 K; (triangle) 1223 K

where $V_m^T/\text{cm}^3 \text{ mol}^{-1}$ is molar volume of a mixture at certain temperature and x_j , x_i are molar fractions of $(\text{LiF-CaF}_2)_{\text{eut.}}$ and SmF_3 , respectively. It is evident that the compressibility parameter for SmF_3 in $(\text{LiF-CaF}_2)_{\text{eut.}}-\text{SmF}_3$ system will be negative and the volume contraction plays a dominant role at concentrations close to pure $(\text{LiF-CaF}_2)_{\text{eut.}}$. The problem to determine its value arises from the fact that the molar volume concentration dependence at low SmF_3 concentrations can be mathematically described by many different ways. It means that one can take the first two, three, four, or more points and use any “suitable” mathematical function. Exactly, the selection of this “suitable” mathematical function plays the crucial role in the final value of partial molar volume of SmF_3 at its

concentration close to zero (representing the situation that one mole of SmF_3 is added to a huge amount of $(\text{LiF-CaF}_2)_{\text{eut.}}$ solvent). The results can vary extremely from smaller positive values to large negative ones. For example, when considering only the first two points of molar volume (at 1123 K) to construct linear function on concentration, a value of partial molar volume as high as $7.5 \text{ cm}^3 \text{ mol}^{-1}$ can be calculated, while for the first four or five points using quadratic function partial molar volumes adopt the values -18.0 or $9.9 \text{ cm}^3 \text{ mol}^{-1}$, respectively. Also other functions could be selected, but one must keep in mind that some of them will not be consistent with physical observation, i.e. some polynomial function of higher power might have increasing character with very small SmF_3 concentration (approaching zero). At this “zero” point, it is crucial whether tangent to the molar volume function will have negative or positive value. This extremely sensitive mathematical function selection influence on calculated values makes impossible to distinguish which function is the right one. However, decrease in molar volume itself with initial SmF_3 addition refers to the volume contraction. It is expected that very compact SmF_3 solid phase, in which each Sm atom is coordinated by nine fluorine atoms, will decompose and its volume will increase during dissolving in $(\text{LiF-CaF}_2)_{\text{eut.}}$. However, the formed components will have strong tendency to make coordination bonds with free F^- anions from ionic $(\text{LiF-CaF}_2)_{\text{eut.}}$, thus resulting to the volume contraction. The final effect will then result in overall volume contraction as a result of the two described opposite processes. If this process would continue at any SmF_3 composition, the concentration of free F^- would continuously decrease and logically it can be expected that the activity of free Li^+ (or Ca^{2+}) cations would increase. Consequently, the formation of ternary compound (e.g. LiSmF_3) will be expected what seems not to be the case. As molar volume increases with further addition of SmF_3 , some other process probably will dominate, but based on only volume properties they cannot be identified and some more sophisticated experiments would be necessary, e.g. in situ EXAFS measurements or others.

In order to, at least, estimate partial molar volume, a series of calculation was done with different input conditions and using both simple linear or polynomial regression and multicomponent polynomial regression. In the late case, an approach of Redlich-Kister equation was used (described in e.g. [19]). Least square parameters minimisation procedure was used for all case. Results are summarised in Table 5. Other combinations provided somehow physically inconsistent results. Finally, it can be estimated that the compressibility parameter will adopt values ca in the interval from -30 to $-40 \text{ cm}^3 \text{ mol}^{-1}$ in the investigated temperature range.

Table 5 Molar volume $V_m^T/\text{cm}^3 \text{mol}^{-1}$ and partial molar volume $\bar{V}_i^T/\text{cm}^3 \text{mol}^{-1}$ of $(\text{LiF}-\text{CaF}_2)_{\text{eut.}}-\text{SmF}_3$ at 1123, 1173, and 1223 K; x_1 is $(\text{LiF}-\text{CaF}_2)_{\text{eut.}}$; x_2 is SmF_3

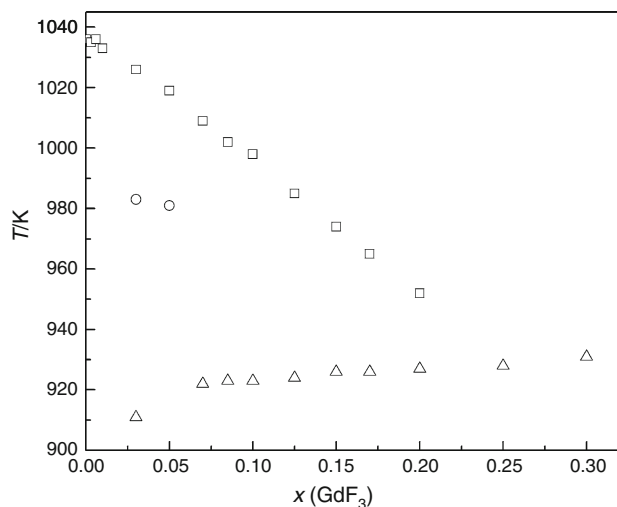
Conditions	$V_m^T/\text{cm}^3 \text{mol}^{-1}$	$\bar{V}_i^T/\text{cm}^3 \text{mol}^{-1}$	$\bar{V}_i^T/\text{cm}^3 \text{mol}^{-1}$ if $x_1 \rightarrow 1$
First two-point simple linear regression	$V_m^{1123\text{K}} = 17.8 - 10.3x_2$ $V_m^{1173\text{K}} = 18.1 - 17.1x_2$ $V_m^{1223\text{K}} = 18.4 - 24.2x_2$	–	$\bar{V}_{\text{SmF}_3}^{1123\text{K}} = 7.5$ $\bar{V}_{\text{SmF}_3}^{1173\text{K}} = 1.0$ $\bar{V}_{\text{SmF}_3}^{1223\text{K}} = -5.8$
First five-point simple quadratic regression	$V_m^{1123\text{K}} = 17.8 - 8.0x_2 + 620.6x_2^2$ $V_m^{1173\text{K}} = 18.0 - 12.3x_2 + 648.6x_2^2$ $V_m^{1223\text{K}} = 18.3 - 16.8x_2 + 679.3x_2^2$	$\bar{V}_{\text{SmF}_3}^{1123\text{K}} = 630.5 - 620.6x_1^2$ $\bar{V}_{\text{SmF}_3}^{1173\text{K}} = 654.4 - 648.6x_1^2$ $\bar{V}_{\text{SmF}_3}^{1223\text{K}} = 680.7 - 679.3x_1^2$	$\bar{V}_{\text{SmF}_3}^{1123\text{K}} = 9.9$ $\bar{V}_{\text{SmF}_3}^{1173\text{K}} = 5.8$ $\bar{V}_{\text{SmF}_3}^{1223\text{K}} = 1.4$
First five-point multicomponent polynomial regression—Redlich–Kister equation	$V_m^{1123\text{K}} = 17.8x_1 + 690.1x_1x_2^2 + 8.9x_1^2x_2$ $V_m^{1173\text{K}} = 18.0x_1 + 714.2x_1x_2^2 + 4.7x_1^2x_2$ $V_m^{1223\text{K}} = 18.3x_1 + 740.5x_1x_2^2 + 0.3x_1^2x_2$	$\bar{V}_{\text{SmF}_3}^{1123\text{K}} = 1371.4x_1^2 - 1362.4x_1^3$ $\bar{V}_{\text{SmF}_3}^{1173\text{K}} = 1423.6x_1^2 - 1418.9x_1^3$ $\bar{V}_{\text{SmF}_3}^{1223\text{K}} = 1480.7x_1^2 - 1480.4x_1^3$	$\bar{V}_{\text{SmF}_3}^{1123\text{K}} = 9.0$ $\bar{V}_{\text{SmF}_3}^{1173\text{K}} = 4.7$ $\bar{V}_{\text{SmF}_3}^{1223\text{K}} = 0.3$

Table 6 Melt composition (x) of GdF_3 , temperatures of primary crystallisation (T_{PC}), together with temperatures of other thermal effects (T_1 , T_2) and hitting temperature (T_{max}) of the $(\text{LiF}-\text{CaF}_2)_{\text{eut.}}-\text{GdF}_3$ system

$x(\text{GdF}_3)$	T_{PC}/K	T_1/K	T_2/K	T_{max}/K
0.000	1036			1073
0.003	1035			1123
0.006	1036			1123
0.010	1033			1103
0.030	1026	983	911	1000
0.050	1019	981		1083
0.070	1009		922	1123
0.085	1002		923	1123
0.100	998		923	1123
0.125	985		924	1123
0.150	974		926	1123
0.170	965		926	1033
0.200	952		927	1033
0.250			928	1033
0.300			931	1173

$(\text{LiF}-\text{CaF}_2)_{\text{eut.}}-\text{GdF}_3$ system

The situation in this system is in some aspects similar to the previous one. Table 6 summarises the temperatures of primary crystallisation together with temperatures of other thermal effects, and data are graphically shown in Fig. 7. The system $\text{LiF}-\text{GdF}_3$ is not simple binary one, and the formation of unspecified crystallisation fields was suggested [23]; moreover, the formation of LiGdF_4 phase was reported in PDF2 database [34]. System $\text{CaF}_2-\text{GdF}_3$ shows

**Fig. 7** Schematic phase diagram of the system $(\text{LiF}-\text{CaF}_2)_{\text{eut.}}-\text{GdF}_3$ with thermal effects: T_{PC} (square), T_1 (circle), T_2 (triangle): molar fraction of GdF_3 (x)

similar features as that one with SmF_3 : formation of different unspecified solid solution areas [26, 27, 35]. In contrast to the system $\text{CaF}_2-\text{SmF}_3$, the formation of additional phase $\text{CaGd}_3\text{F}_{11}$ was reported in the system $\text{CaF}_2-\text{GdF}_3$, as well as the formation of $\text{Ca}_{0.2}\text{Gd}_{0.8}\text{F}_{2.8}$ [36] and $\text{Ca}_{0.88}\text{Gd}_{0.12}\text{F}_{2.12}$ phases [37]. Measured experimental data of primary crystallisation temperatures indicate to existence of simple binary system; however, it is probably not the case and these data represent similar situation as in the system above, i.e. the formation of solid solution fields. This increased tendency to form additional phases is visible also from analysis of XRD patterns of the solidified

Table 7 Phases identified in the XRD patterns of the solidified samples of the (LiF–CaF₂)_{eut.}–GdF₃ system

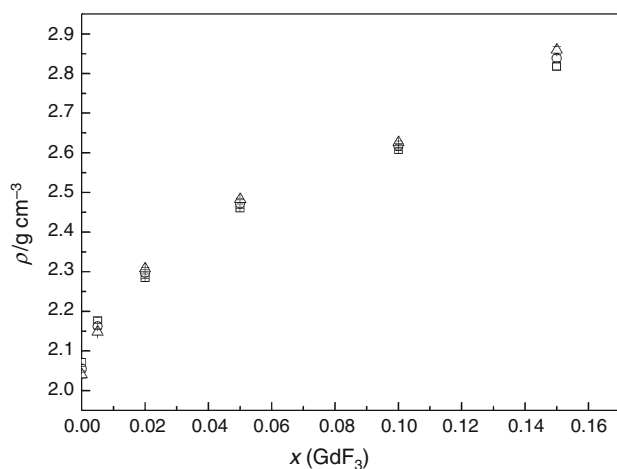
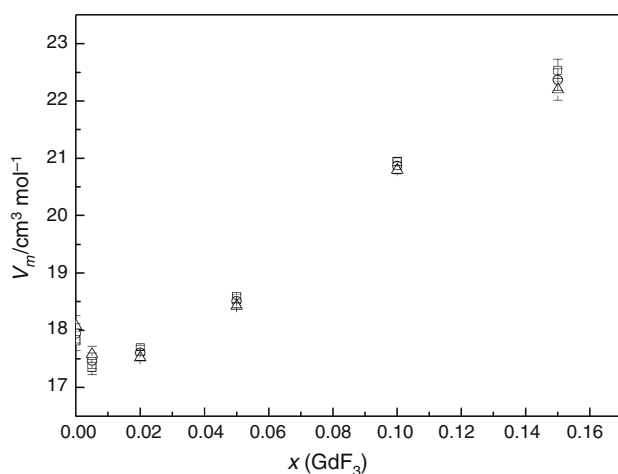
$x(\text{GdF}_3)$	$w(\text{GdF}_3)$	LiF	CaF ₂	GdF ₃	GdOF	LiGdF ₄	Unassigned diffractions $d/\text{Å}$
1.000	1.000	–	–	+	–	–	4.1416
0.010	0.055	+	+	–	+	–	1.9636 1.6617
0.030	0.152	+	+	–	+	+	4.1431 2.7771
0.050	0.234	+	+	–	+	+	2.7769
0.100	0.392	+	–	–	+	+	4.1337 2.7749 1.7169 1.5988 1.5302 1.5016
0.125	0.454	+	–	–	–	+	3.2001 2.7748 1.7173 1.6713 1.6005 1.5307 1.5020 1.4343
0.150	0.506	+	–	–	–	+	4.1376 3.2078 2.7792 1.9597 1.7182 1.6761 1.6707 1.6008
0.170	0.543	+	–	–	–	+	3.2062 2.7771 1.7179 1.6744 1.6044 1.5995
0.200	0.592	+	–	–	–	+	3.2071 2.7767 1.7171 1.6750 1.6038 1.5987 1.5306 1.5018 1.4342

samples summarised in Table 7. The presence of GdF₃ was not observed as the most probably it reacts with either LiF or CaF₂ or both. The formation of other phases (unidentified) is also highly probable as some unidentified

diffractions were observed in solidified samples and their intensity change with concentration variation. Solid–solid phase transformation of pure GdF₃ was reported at temperature 1172 K [38] or at 1310 K [22].

Table 8 Regression coefficients $a/\text{g cm}^{-3}$ and $b/\text{g cm}^{-3} \text{K}^{-1}$ and their the standard deviations for the temperature (T/K) dependence of the density ($\rho/\text{g cm}^{-3}$) of the investigated system $(\text{LiF-CaF}_2)_{\text{eut.}}\text{-GdF}_3$

$x(\text{LiF-CaF}_2)_{\text{eut.}}$	$x(\text{GdF}_3)$	$a/\text{g cm}^{-3}$	$b \times 10^4/\text{g cm}^{-3} \text{K}^{-1}$	T/K
1.000	0.000	2.758 ± 0.007	6.119 ± 0.059	1203–1073
0.995	0.005	2.811 ± 0.006	5.646 ± 0.048	1223–1123
0.980	0.020	1.788 ± 0.002	-4.430 ± 0.017	1133–1033
0.950	0.050	1.974 ± 0.001	-4.339 ± 0.011	1223–1023
0.900	0.100	2.199 ± 0.002	-3.647 ± 0.020	1173–1033
0.850	0.150	1.872 ± 0.006	-8.417 ± 0.054	1123–1023

**Fig. 8** Graphical representation of concentration dependence of the density ρ and the standard deviations of ρ of the molten system $(\text{LiF-CaF}_2)_{\text{eut.}}\text{-GdF}_3$ at temperature (square) 1123 K; (circle) 1148 K; (triangle) 1173 K**Fig. 9** Molar volume V_m and the standard deviation of V_m of the molten system $(\text{LiF-CaF}_2)_{\text{eut.}}\text{-GdF}_3$ at temperatures (square) 1123 K; (circle) 1148 K; (triangle) 1173 K

Concerning the volume properties, Table 8 summarises the regression coefficients a and b for calculation of density of the $(\text{LiF-CaF}_2)_{\text{eut.}}\text{-GdF}_3$ system and concentration dependence of density calculated based on these coefficients is shown in Fig. 8. The main difference in comparison with the previous system is that the density increases with temperature over 0.02 mol % addition of GdF_3 . This is anomalous behaviour in contrast to the majority of the systems when density decreases with increasing temperature.

Some more information can be deduced from volume properties, Fig. 9. We are not aware of any data neither for binary systems LiF-GdF_3 and $\text{CaF}_2\text{-GdF}_3$ nor for the quasi-binary system $(\text{LiF-CaF}_2)_{\text{eut.}}\text{-GdF}_3$. Volume properties were treated in similar way as for samarium analogue system. With initial addition of GdF_3 ($x = 0.05$), values of molar volume decrease, and values of molar volume increase with increasing temperature as was expected and as was observed also for pure $(\text{LiF-CaF}_2)_{\text{eut.}}$ and all points in the system $(\text{LiF-CaF}_2)_{\text{eut.}}\text{-SmF}_3$. With further addition of GdF_3 , molar volume increases like in samarium analogous system; however, the values of molar volume decrease with temperature at particular concentrations. This is significantly different behaviour from the previous system. Reason for these observations is unknown and might arise from the structural properties of gadolinium salt. In spite of these obstacles, partial molar volumes were calculated analogously to samarium system and are summarised in Table 9. As can be seen, partial molar volumes have relatively large negative values at higher temperatures, ca $-30 \text{ cm}^3 \text{mol}^{-1}$. From these values, an unusual consequence can be deduced at higher temperatures. When one mole of GdF_3 at e.g. 1173 K (it is in solid state at this temperature and its molar volume is expected to be relatively close to its value at room temperature that is $30.4 \text{ cm}^3 \text{mol}^{-1}$) is added to the large amount of molten $(\text{LiF-CaF}_2)_{\text{eut.}}$, the final volume of the system will even decrease; this can be quantified by compressibility factor ζ ca $-60 \text{ cm}^3 \text{mol}^{-1}$. Of course, it is valid only at low

Table 9 Molar volume $V_m^T/\text{cm}^3 \text{mol}^{-1}$ and partial molar volume $\bar{V}_i^T/\text{cm}^3 \text{mol}^{-1}$ of (LiF–CaF₂)_{eut.}–GdF₃ at 1123, 1173, and 1223 K; x_1 is (LiF–CaF₂)_{eut.}; x_2 is GdF₃

Conditions	$V_m^T/\text{cm}^3 \text{mol}^{-1}$	$\bar{V}_i^T/\text{cm}^3 \text{mol}^{-1}$	$\bar{V}_i^T/\text{cm}^3 \text{mol}^{-1}$ if $x_2 \rightarrow 1$
First two-point simple linear regression	$V_m^{1123\text{K}} = 17.8 - 91.2x_2$ $V_m^{1148\text{K}} = 17.9 - 95.1x_2$ $V_m^{1173\text{K}} = 18.1 - 99.0x_2$	–	$\bar{V}_{\text{GdF}_3}^{1123\text{K}} = -73.4$ $\bar{V}_{\text{GdF}_3}^{1148\text{K}} = -77.2$ $\bar{V}_{\text{GdF}_3}^{1173\text{K}} = -80.9$
First four-point simple quadratic regression	$V_m^{1123\text{K}} = 17.7 - 16.9x_2 + 717.9x_2^2$ $V_m^{1148\text{K}} = 17.8 - 32.7x_2 + 938.8x_2^2$ $V_m^{1173\text{K}} = 18.0 - 48.6x_2 + 1160.8x_2^2$	$\bar{V}_{\text{GdF}_3}^{1123\text{K}} = 718.7 - 717.9x_1^2$ $\bar{V}_{\text{GdF}_3}^{1148\text{K}} = 923.9 - 938.8x_1^2$ $\bar{V}_{\text{GdF}_3}^{1173\text{K}} = 1130.2 - 1160.8x_1^2$	$\bar{V}_{\text{GdF}_3}^{1123\text{K}} = 0.8$ $\bar{V}_{\text{GdF}_3}^{1148\text{K}} = -14.9$ $\bar{V}_{\text{GdF}_3}^{1173\text{K}} = -30.6$
First four-point multicomponent polynomial regression—Redlich–Kister equation	$V_m^{1123\text{K}} = 17.7x_1 + 774.0x_1x_2 - 774.0x_1^2x_2$ $V_m^{1148\text{K}} = 17.8x_1 + 975.5x_1x_2^2 - 15.8x_1^2x_2$ $V_m^{1173\text{K}} = 18.0x_1 + 117.8x_1x_2^2 - 31.6x_1^2x_2$	$\bar{V}_{\text{GdF}_3}^{1123\text{K}} = 1547.9x_1^2 - 1548.0x_1^3$ $\bar{V}_{\text{GdF}_3}^{1148\text{K}} = 1966.7x_1^2 - 1982.4x_1^3$ $\bar{V}_{\text{GdF}_3}^{1173\text{K}} = 267.2x_1^2 - 298.8x_1^3$	$\bar{V}_{\text{GdF}_3}^{1123\text{K}} = -0.1$ $\bar{V}_{\text{GdF}_3}^{1148\text{K}} = -15.7$ $\bar{V}_{\text{GdF}_3}^{1173\text{K}} = -31.6$

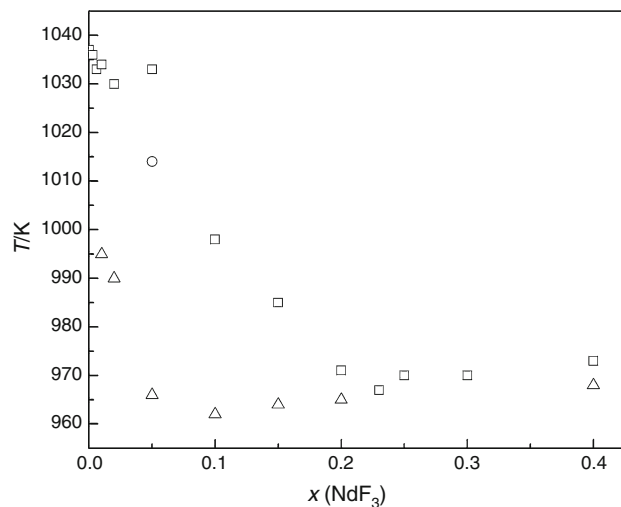
Table 10 Melt composition (x) of NdF₃, temperatures of primary crystallisation (T_{PC}), together with temperatures of other thermal effects (T_1 , T_2) and hitting temperature ($T_{\text{max.}}$) of the (LiF–CaF₂)_{eut.}–NdF₃ system

$x(\text{NdF}_3)$	T_{PC}/K	T_1/K	T_2/K	$T_{\text{max.}}/\text{K}$
0.000	1037			1073
0.003	1036			1073
0.006	1033			1093
0.010	1034		995	1093
0.020	1030		990	1093
0.050	1033	1014	966	1093
0.100	998		962	1093
0.150	985		964	1093
0.200	971		965	1093
0.230	967			1163
0.250	970			1203
0.300	970			1223
0.400	973		968	1223

concentration below 2 mol % of GdF₃. This observation has interesting impact to the practical application when addition of small portions of GdF₃ to the certain melts will have not to be compensated by larger volume of pots.

(LiF–CaF₂)_{eut.}–NdF₃ system

Table 10 summarises the temperatures of primary crystallisation together with temperatures of other thermal effects, and data are graphically shown in Fig. 10. This system is more similar to the system (LiF–CaF₂)_{eut.}–SmF₃ as to the gadolinium analogue. Based on literature data, the

**Fig. 10** Schematic phase diagram of the system (LiF–CaF₂)_{eut.}–NdF₃ with thermal effects: T_{PC} (square), T_1 (circle), T_2 (triangle): molar fraction of NdF₃ (x)

binary system LiF–NdF₃ seems to be simple binary system without the formation of additional phases [23]; however, some ternary phases were identified in the systems MF–NdF₃ (M = Na, K, Rb) [24, 39, 40]. Binary system CaF₂–NdF₃ shows features of solid solution areas formation [26, 27].

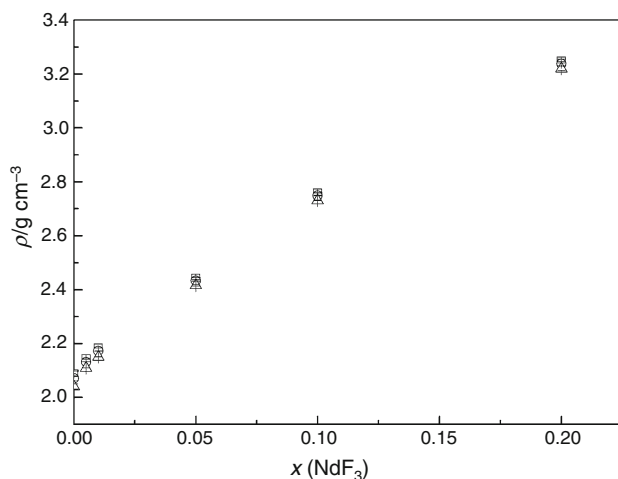
Measured experimental data of primary crystallisation indicate the existence of simple binary system; however, it is probably not the case and these data represent similar situation as was described in both systems above i.e. the formation of solid solution fields. XRD patterns of solidified samples are summarised in Table 11. It is

Table 11 Phases identified in the XRD patterns of the solidified samples of the $(\text{LiF}-\text{CaF}_2)_{\text{eut.}}-\text{NdF}_3$ system

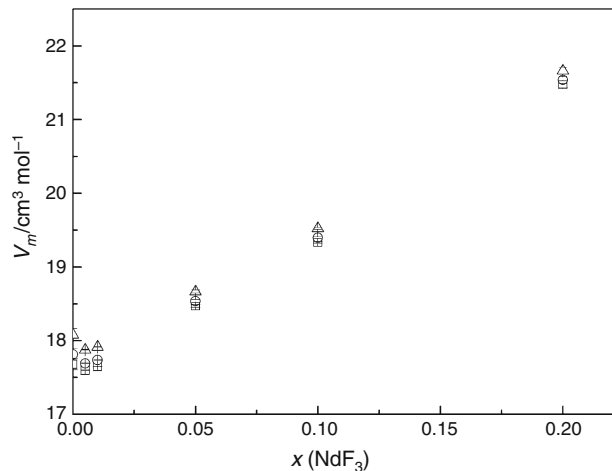
$x(\text{NdF}_3)$	$w(\text{NdF}_3)$	LiF	CaF_2	NdF_3	NdOF	Unassigned diffractions $d/\text{Å}$
0.010	0.052	+	+	−	+	−
0.050	0.223	+	+	−	+	−
0.100	0.377	+	−	+	+	−
0.200	0.577	+	−	+	+	−
0.250	0.645	+	−	+	+	−
0.300	0.700	+	−	+	+	−
0.400	0.784	+	−	+	−	3.2655 2.8281

Table 12 Regression coefficients $a/\text{g cm}^{-3}$ and $b/\text{g cm}^{-3} \text{K}^{-1}$ and the standard deviations for the temperature (T/K) dependence of the density ($\rho/\text{g cm}^{-3}$) of the investigated system $(\text{LiF}-\text{CaF}_2)_{\text{eut.}}-\text{NdF}_3$

$x(\text{LiF}-\text{CaF}_2)_{\text{eut.}}$	$x(\text{NdF}_3)$	$a/\text{g cm}^{-3}$	$b \times 10^4/\text{g cm}^{-3} \text{K}^{-1}$	T/K
1.000	0.000	2.758 ± 0.007	6.119 ± 0.059	1203–1073
0.995	0.005	2.630 ± 0.004	4.436 ± 0.003	1223–1053
0.990	0.010	2.662 ± 0.003	4.361 ± 0.002	1223–1063
0.950	0.050	2.817 ± 0.002	3.415 ± 0.016	1213–1073
0.900	0.100	3.151 ± 0.001	3.578 ± 0.011	1173–1043
0.800	0.200	3.652 ± 0.005	3.682 ± 0.043	1223–1093

**Fig. 11** Graphical representation of concentration dependence of the density ρ and the standard deviations of ρ of the molten system $(\text{LiF}-\text{CaF}_2)_{\text{eut.}}-\text{NdF}_3$ at temperature (square) 1098 K; (circle) 1123 K; (triangle) 1173 K

evident that Nd system shows similar features like Sm system; only initial phases in solidified samples were identified (together with some NdOF impurities), and the formation of any other known ternary fluorides was observed, in contrast to Gd system. However, the presence of unidentified diffractions indicates the formation of

**Fig. 12** Molar volume V_m and the standard deviation of V_m of the molten system $(\text{LiF}-\text{CaF}_2)_{\text{eut.}}-\text{NdF}_3$ at temperatures (square) 1098 K; (circle) 1123 K; (triangle) 1173 K

some new phases. These new phases in all three cases require deeper analysis that is, however, beyond the scope of this work

We are not aware of solid–solid phase transformation of pure NdF_3 (in contrast to published data for SmF_3 and GdF_3).

Table 13 Molar volume $V_m^T/\text{cm}^3 \text{mol}^{-1}$ and partial molar volume $\bar{V}_i^T/\text{cm}^3 \text{mol}^{-1}$ of (LiF–CaF₂)_{eut.}–NdF₃ at 1098, 1123, and 1173 K; x_1 is (LiF–CaF₂)_{eut.}; x_2 is NdF₃

Conditions	$V_m^T/\text{cm}^3 \text{mol}^{-1}$	$\bar{V}_i^T/\text{cm}^3 \text{mol}^{-1}$	$\bar{V}_i^T/\text{cm}^3 \text{mol}^{-1}$ if $x_2 \rightarrow 1$
First two-point simple linear regression	$V_m^{1098 \text{ K}} = 17.7 - 16.5x_2$ $V_m^{1123 \text{ K}} = 17.8 - 24.3x_2$ $V_m^{1173 \text{ K}} = 18.1 - 40.5x_2$	–	$\bar{V}_{\text{NdF}_3}^{1098 \text{ K}} = 1.2$ $\bar{V}_{\text{NdF}_3}^{1123 \text{ K}} = -6.5$ $\bar{V}_{\text{NdF}_3}^{1173 \text{ K}} = -22.4$
First four-point simple quadratic regression	$V_m^{1098 \text{ K}} = 17.7 - 8.7x_2 + 497.1x_2^2$ $V_m^{1123 \text{ K}} = 17.8 - 13.8x_2 + 574.8x_2^2$ $V_m^{1173 \text{ K}} = 18.0 - 24.4x_2 + 736.3x_2^2$	$\bar{V}_{\text{NdF}_3}^{1098 \text{ K}} = 506.1 - 497.1x_1^2$ $\bar{V}_{\text{NdF}_3}^{1123 \text{ K}} = 578.8 - 574.8x_1^2$ $\bar{V}_{\text{NdF}_3}^{1173 \text{ K}} = 729.9 - 736.3x_1^2$	$\bar{V}_{\text{NdF}_3}^{1098 \text{ K}} = 9.0$ $\bar{V}_{\text{NdF}_3}^{1123 \text{ K}} = 4.0$ $\bar{V}_{\text{NdF}_3}^{1173 \text{ K}} = -6.4$
First four-point multicomponent polynomial regression—Redlich–Kister equation	$V_m^{1098 \text{ K}} = 17.7x_1 + 545.9x_1x_2^2 + 8.7x_1^2x_2$ $V_m^{1123 \text{ K}} = 17.8x_1 + 619.9x_1x_2^2 + 3.6x_1^2x_2$ $V_m^{1173 \text{ K}} = 18.0x_1 - 6.7x_1x_2 + 775.8x_1x_2^2$	$\bar{V}_{\text{NdF}_3}^{1098 \text{ K}} = 1083.1x_1^2 - 1074.4x_1^3$ $\bar{V}_{\text{NdF}_3}^{1123 \text{ K}} = 1236.2x_1^2 - 1232.6x_1^3$ $\bar{V}_{\text{NdF}_3}^{1173 \text{ K}} = 1544.9x_1^2 - 1551.7x_1^3$	$\bar{V}_{\text{NdF}_3}^{1098 \text{ K}} = 8.7$ $\bar{V}_{\text{NdF}_3}^{1123 \text{ K}} = 3.6$ $\bar{V}_{\text{NdF}_3}^{1173 \text{ K}} = -6.8$

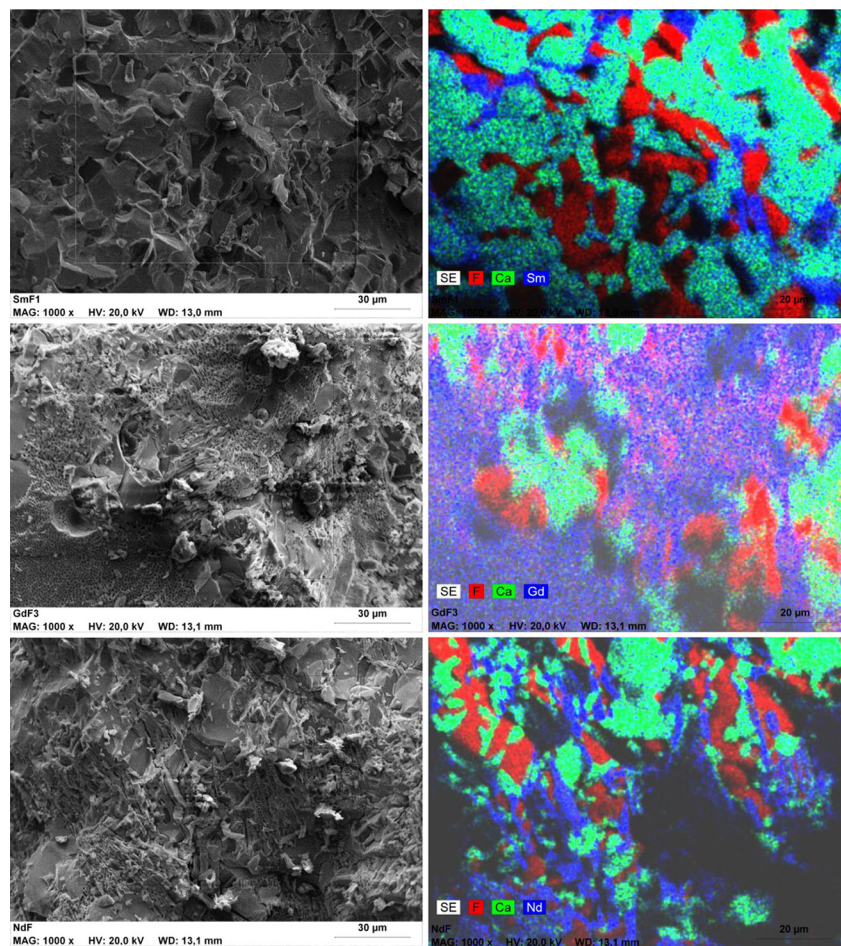
Fig. 13 SEM images of the solidified samples of the systems (LiF–CaF₂)_{eut.}–20 mol % LnF₃ (Ln = Sm, Gd, and Nd) from top to down (*left*) and element mapping (*right*)

Table 12 summarises the regression coefficients a and b for calculation of density of the (LiF–CaF₂)_{eut.}–NdF₃ system. Data from density measurements (see Fig. 11)

show similar features to the previous both systems resulting to the analogous behaviour also of volume properties. These are, however, more close to samarium system

(without anomalous behaviour of molar volume) like in gadolinium system (i.e. values of molar volume decreases with temperature at certain concentration). Molar volume shows local minimum (see Fig. 12) at low NdF_3 concentrations, like in Sm and Gd systems. When comparing values of all three systems, molar volume of Nd system at e.g. 15 mol % at 1123 K is lowest in the series $\text{Nd} < \text{Sm} < \text{Gd}$ what obeys the elements position in the periodic table (but does not obey the sequence of molar volumes of tri-fluorides in solid state that is $\text{Gd} < \text{Nd} < \text{Sm}$).

Partial molar volumes of NdF_3 were treated like in samarium and gadolinium analogues and are summarised in Table 13. As can be seen, partial molar volumes of NdF_3 and SmF_3 in $(\text{LiF}-\text{CaF}_2)_{\text{eut}}$ are closer to each other at comparable temperatures as partial molar volume of GdF_3 that is significantly lower.

SEM EDX analysis

From the SEM images of the solidified samples (Fig. 13), it can be seen that morphology of samarium samples seems to be slightly different from those of gadolinium and neodymium; however, the expected homogeneity seems to be present in all studied systems. Based on the element mapping, it can be deduced that mixtures of crystalline phases with different compositions of grains are present. This observation is in agreement with XRD result confirming the crystalline nature of samples (with some degree of glassy phase). Both SEM images and EDX mapping provide supporting information to XRD results, i.e. features of solid solution formation can be deduced from diffusive boundaries of element contents between particular grains.

Conclusions

Temperatures of primary crystallisation of the systems $(\text{LiF}-\text{CaF}_2)_{\text{eut}}-\text{LnF}_3$ ($\text{Ln} = \text{Sm}, \text{Gd}, \text{and Nd}$) were measured in order to provide, at least, scheme of phase diagrams. Based on XRD patterns of solidified samples, it can be expected that some new phases are formed in all three systems. The number of these phases, however, cannot be predicted. In spite of the effort, several procedures to obtain suitable single crystals for their structural characterisation have failed.

Volume properties analysis revealed unusual behaviour of investigated systems, in some aspect even anomalous. Small additions of LnF_3 up to 1 mol % to $(\text{LiF}-\text{CaF}_2)_{\text{eut}}$ result in decrease in molar volume. This has consequence to the partial molar volumes of LnF_3 thus having very small even negative values at higher temperatures. Such a

relatively large volume contraction, when expressed through the compressibility parameter, may reach values that are bigger (in absolute value) than molar volume of pure component.

Samarium and neodymium systems show similar properties in phase analysis, as well as in volume properties, while gadolinium system shows different behaviours. The reason for this macroscopic behaviour could arise from the structural and electronic properties of the central atoms. The main difference between the studied three systems is that Nd^{3+} and Sm^{3+} have similar electronic properties in the sense of only partially occupied f orbitals, while Gd^{+3} has f orbitals fully half filled. These different microscopic properties might result also to the different macroscopic ones. In order to prove this hypothesis, more extended experiments are required including also other lanthanides.

Acknowledgements This work was supported by the Science and Technology Assistance Agency under contract No. APVV-0460-10 and by the Slovak Grant Agency VEGA 2/0116/14 and VEGA 2/0095/12. This contribution/publication is the result of the project implementation: “Centre for materials, layers and systems for applications and chemical processes under extreme conditions—Stage II”, ITMS code 26240120021, supported by the Research & Development Operational Programme funded by the ERDF.

References

1. Fernández AG, Galleguillos H, Fuentealba E, Pérez FJ. Thermal characterization of HITEC molten salt for energy storage in solar linear concentrated technology. *J Therm Anal Calorim.* 2015;122(1):3–9. doi:10.1007/s10973-015-4715-9.
2. Peng Q, Yang X, Ding J, Wei X, Yang J. Thermodynamic performance of the $\text{NaNO}_3-\text{NaCl}-\text{NaNO}_2$ ternary system. *J Therm Anal Calorim.* 2013;115(2):1753–8. doi:10.1007/s10973-013-3389-4.
3. Wang J, Lai M, Han H, Ding Z, Liu S, Zeng D. Thermodynamic modeling and experimental verification of eutectic point in the $\text{LiNO}_3-\text{KNO}_3-\text{Ca}(\text{NO}_3)_2$ ternary system. *J Therm Anal Calorim.* 2014;119(2):1259–66. doi:10.1007/s10973-014-4218-0.
4. Thoma RE. Rare—earth halides. Tennessee: Oak Ridge National Laboratory Reactor Chemistry Division, U.S. Atomic Energy Commission, Oak Ridge National Laboratory 1965.
5. Capelli E, Benes O, Beilmann M, Konings RJM. Thermodynamic investigation of the $\text{LiF}-\text{ThF}_4$ system. *J Chem Thermodyn.* 2013;58:110–6. doi:10.1016/j.jct.2012.10.013.
6. Barborík P, Vasková Z, Boča M, Priščák J. Physicochemical properties of the system $(\text{LiF} + \text{NaF} + \text{KF}_{(\text{eut.})} + \text{Na}_7\text{Zr}_6\text{F}_{31})$: phase equilibria, density and volume properties, viscosity and surface tension. *J Chem Thermodyn.* 2014;76:145–51. doi:10.1016/j.jct.2014.03.024.
7. Boca M, Danielik V, Ivanova Z, Miksikova E, Kubikova B. Phase diagrams of the $\text{KF}-\text{K}_2\text{TaF}_7$ and $\text{KF}-\text{Ta}_2\text{O}_5$ systems. *J Therm Anal Calorim.* 2007;90:159–65. doi:10.1007/s10973-006-7700-5.
8. Chrenkova M, Danielik V, Kubikova B, Danek V. CALPHAD: phase diagram of the system $\text{LiF}-\text{NaF}-\text{K}_2\text{NbF}_7$. *Calphad-Computer Coupling of Phase Diagrams and Thermochemistry.* 2003;27(1):19–26. doi:10.1016/s0364-5916(03)00027-0.

9. Dvorak V, Danielik V, Matal O, Chrenkova M, Boca M. Phase diagram of the system $\text{NaF}-\text{SnF}_2$. *J Therm Anal Calorim.* 2008;91(2):541–4. doi:10.1007/s10973-006-8320-9.
10. Kubikova B, Danek V, Gaune-Escard M. Phase equilibria in the molten system $\text{KF}-\text{K}_2\text{NbF}_7-\text{Nb}_2\text{O}_5$. *Zeitschrift Fur Physikalische Chemie-Int J Res Phys Chem Chem Phys.* 2006;220(6):765–73. doi:10.1007/s10967-014-3100-7.
11. Kubikova B, Kucharik M, Vasiljev R, Boca M. Phase equilibria, volume properties, surface tension, and viscosity of the $(\text{FLiNaK})_{\text{eut.}} + \text{K}_2\text{NbF}_7$ Melts. *J Chem Eng Data.* 2009;54(7):2081–4. doi:10.1021/je800979q.
12. Kubikova B, Mackova I, Boca M. Phase analysis and volume properties of the $(\text{LiF}-\text{NaF}-\text{KF})_{\text{eut.}}-\text{K}_2\text{ZrF}_6$ system. *Monatshefte Fur Chemie.* 2013;144(3):295–300. doi:10.1007/s00706-012-0886-2.
13. Kubíková B, Mlynáriková J, Vasková Z, Jeřábková P, Boča M. Phase analysis and density of the system $\text{K}_2\text{ZrF}_6-\text{K}_2\text{TaF}_7$. *Monatshefte für Chemie – Chem Monthly.* 2014;145(8):1247–52. doi:10.1007/s00706-014-1214-9.
14. Simko F, Danek V. Cryoscopy in the system $\text{Na}_3\text{AlF}_6-\text{Fe}_2\text{O}_3$. *Chem Papers-Chem Zvesti.* 2001;55(5):269–72.
15. Silny A. Zariadenie na meranie hustoty kvapalín. *Sdelovaci Technika.* 1990;38:101–5.
16. Boca M, Ivanova Z, Kucharik M, Cibulkova J, Vasiljev R, Chrenkova M. Density and surface tension of the system $\text{KF}-\text{K}_2\text{TaF}_7-\text{Ta}_2\text{O}_5$. *Zeitschrift Fur Physikalische Chemie-Int J Res Phys Chem Chem Phys.* 2006;220(9):1159–80. doi:10.1524/zpch.2006.220.9.1159.
17. Chrenkova M, Boca M, Kucharik M, Danek V. Density of melts of the system $\text{KF}-\text{K}_2\text{MoO}_4-\text{SiO}_2$. *Chem Papers-Chem Zvesti.* 2002;56(5):283–7.
18. Cibulkova J, Chrenkova M, Boca M. Density of the system $\text{KF} + \text{K}_2\text{NbF}_7 + \text{Nb}_2\text{O}_5$. *J Chem Eng Data.* 2005;50(2):477–80. doi:10.1021/je049702k.
19. Cibulkova J, Chrenkova M, Vasiljev R, Kremenetsky V, Boca M. Density and viscosity of the $(\text{LiF} + \text{NaF} + \text{KF})_{\text{eut.}}(1) + \text{K}_2\text{TaF}_7(2) + \text{Ta}_2\text{O}_5(3)$ melts. *J Chem Eng Data.* 2006;51(3):984–7. doi:10.1021/je050490g.
20. Kostenska I, Vrbenska J, Malinovsky M. The equilibrium “solidus—liquidus” in the system lithium fluoride—calcium fluoride. *Chem Zvesti.* 1974;28(4):531–8.
21. Roake WE. The Systems CaF_2-LiF and $\text{CaF}_2-\text{LiF}-\text{MgF}_2$. *J Electrochem Soc.* 1957;104(11):661–2.
22. Stankus SV, Khairulin RA, Lyapunov KM. Thermal properties and phase transitions of heavy rare-earth fluorides. *High Temp High Pressures.* 2000;32:467–72. doi:10.1068/htwu216.
23. Thoma RE, Brunton GD, Penneman RA, Keenan TK. Equilibrium relations and crystal structure of lithium fluorolanthanate phases. *Inorg Chem.* 1970;9(5):1096–100. doi:10.1021/ic50087a019.
24. Thoma RE, Inasley H, Hebert GM. The sodium fluoride-lanthanide trifluoride systems. *Inorg Chem.* 1966;5(7):1222–9. doi:10.1021/ic50041a032.
25. Dergunov EP. Complex formation between fluorides of alkali metals and of lanthanide-group metals. *Dokl Akad Nauk SSSR.* 1952;85(5):1025–8.
26. Sobolev BP, Fedorov PP. Phase diagrams of the $\text{CaF}_2-(\text{Y}, \text{Ln})\text{F}_3$ systems I. Experimental. *J Less-Common Met.* 1978;60(1):33–46.
27. Sobolev BP, Fedorov PP, Seiranyan KB, Tkachenko NL. On the problem of polymorphism and fusion of lanthanide trifluorides. II. Interaction of LnF_3 with MF_2 ($\text{M} = \text{calcium, strontium, barium}$), change in structural type in the LnF_3 series, and thermal characteristics. *J Solid State Chem.* 1976;17(1–2):201–12. doi:10.1016/0022-4596(76)90221-8.
28. Gogadze NG, Ippolitov EG, Zhigarnovskii BM. Liquid and solid phase diagrams of calcium fluoride-samarium fluoride and calcium fluoride-dysprosium fluoride above 800.deg. *Zh Neorg Khim.* 1972;17(2):576–7.
29. Rotereau K, Daniel P, Desert A, Gesland JY. The high-temperature phase transition in samarium fluoride, SmF_3 : structural and vibrational investigation. *J Phys: Condens Matter.* 1998;10(6):1431–46. doi:10.1088/0953-8984/10/6/026.
30. Janz GJ, Tomkins RPT. Physical properties data compilation relevant to energy storage. Washington, DC: National Bureau of Standards; 1981.
31. Vasková Z, Kontrík M, Mlynáriková J, Boča M. Density of low-temperature $\text{KF}-\text{AlF}_3$ Aluminum Baths with Al_2O_3 and AlPO_4 Additives. *Metall Mater Trans B.* 2015;46(1):485–93. doi:10.1007/s11663-014-0218-5.
32. Simko F, Mackova I, Netrova Z. Density of the systems $(\text{NaF}/\text{AlF}_3)-\text{AlPO}_4$ and $(\text{NaF}/\text{AlF}_3)-\text{NaVO}_3$. *Chem Pap.* 2011;65(1):85–9. doi:10.2478/s11696-010-0074-y.
33. Mlynarikova J, Boca M, Kipsova L. The role of the alkaline cations in the density and volume properties of the melts $\text{MF}-\text{K}_2\text{NbF}_7$ ($\text{MF} = \text{LiF}-\text{NaF}, \text{LiF}-\text{KF}$ and $\text{NaF}-\text{KF}$). *J Mol Liq.* 2008;140(1–3):101–7. doi:10.1016/j.molliq.2008.02.002.
34. Brunton GD, Inasley H, McVey TN, Thoma RE. Crystallographic data for some metal fluorides, chlorides, and oxides Oak Ridge Natl. Lab. Rep. ORNL (U.S.) 1965.
35. Fedorov PP, Sizganov YG, Sobolev PP, Shvanner M. Phase diagram of the system $\text{CaF}_2-\text{GdF}_3$. *J Therm Anal.* 1975;8(2):239–45.
36. Otroshchenko LP, Aleksandrov BP, Maksimov BA, Simonov VI, Sobolev BP. Stabilization of the high-symmetric hexagonal form of tysonite in the nonstoichiometric phase gadolinium calcium fluoride ($\text{Gd}_{0.8}\text{Ca}_{0.2}\text{F}_{2.8}$). *Soviet Phys Crystallogr.* 1985;30(4):383–6.
37. Grigor'eva NB, Maksimov BA, Sobolev BP. X-ray diffraction study of $\text{Ca}_{0.88}\text{Gd}_{0.12}\text{F}_{2.12}$ single crystals with a modified fluorite structure. *Crystallogr Rep.* 2000;45(5):718–20.
38. Klimm D, Ranieri IM, Bertram R, Baldochi SL. The phase diagram YF_3-GdF_3 . *Mater Res Bull.* 2008;43:676–81. doi:10.1016/j.materresbull.2007.04.004.
39. Pyrina VK, Prostakov ME. Interaction of potassium tetrafluoroborate with potassium, lanthanum, and neodymium fluorides in a melt. *Zh Neorg Khim.* 1975;20(4):1140–2.
40. Nafikova SK, Reshetnikova LP, Novoselova AV. Rubidium fluoride-neodymium fluoride system. *Zh Neorg Khim.* 1976;21(9):2521–4.